Applied Physics Letters

RESEARCH ARTICLE | JUNE 29 2026

Mn-doping with reduced carry-over effect in semi-insulating GaN grown by MOCVD

Special Collection: Frontiers in Nitride Semiconductors Research

Teresa Duarte ; Patrik Straňák ; Lutz Kirste ; Mario Prescher ; Fouad Benkhelifa ; Byeongchan So ; Stefano Leone ; Patricie Merkert ; Rüdiger Quay

Check for updates

Appl. Phys. Lett. 128, 262102 (2026)
https://doi.org/10.1063/5.0336269

View Online
Export Citation

22 July 2026 14:45:25

AIP Advances
Why Publish With Us?
21DAYS average time to 1st decision
OVER 4 MILLION views in the last year
INCLUSIVE scope
Learn More
AIP Publishing

AIP Publishing

Applied Physics Letters ARTICLE pubs.aip.org/aip/apl

Mn-doping with reduced carry-over effect in semi-insulating GaN grown by MOCVD

Cite as: Appl. Phys. Lett. **128**, 262102 (2026); doi: 10.1063/5.0336269
Submitted: 30 March 2026 · Accepted: 4 June 2026 ·
Published Online: 29 June 2026

View Online Export Citation CrossMark

Teresa Duarte,[a] Patrik Straňák, Lutz Kirste, Mario Prescher, Fouad Benkhelifa, Byeongchan So,[a] Stefano Leone,[a] Patricie Merkert, and Rüdiger Quay

AFFILIATIONS

Fraunhofer Institute for Applied Solid State Physics IAF, 79108 Freiburg, Germany

Note: This paper is part of the Special Topic on Frontiers in Nitride Semiconductors Research.
[a]**Authors to whom correspondence should be addressed:** teresa.duarte@iaf.fraunhofer.de; byeongchan.so@iaf.fraunhofer.de; and leonestefano@hotmail.com

ABSTRACT

Semi-insulating GaN layers for high-electron mobility transistors (HEMTs) used in radio frequency applications are typically achieved through Fe-doping, despite its known adverse effects on transport properties. In this paper, we investigate the possibility of using Mn as an alternative dopant to Fe for GaN buffer layers grown by metal-organic chemical vapor deposition and assess its incorporation onto the subsequent non-intentionally doped (nid) layers. For this purpose, two studies were conducted: first, epitaxial heterostructures for HEMTs were grown with varying the thickness of the nid GaN layer, while keeping the total GaN stack thickness and the Mn-doping level, followed by varying the Mn-doping level and keeping the GaN stack thickness. The Mn-doped buffer layers showed a much faster concentration decay into the subsequent nid GaN layers than Fe. The samples maintained good surface morphology and crystalline quality, and their transport properties did not degrade with different GaN stack thicknesses and doping levels, showcasing Mn as a promising dopant for semi-insulating GaN buffer layers.

© *2026 Author(s). All article content, except where otherwise noted, is licensed under a Creative Commons Attribution (CC BY) license (https://creativecommons.org/licenses/by/4.0/).* https://doi.org/10.1063/5.0336269

22 July 2026 14:45:25

AlGaN/GaN high-electron mobility transistors (HEMTs) exploit the advantage of the spontaneous and piezoelectric polarization naturally occurring at the AlGaN/GaN heterointerface, which induces a highly conductive two-dimensional electron gas (2DEG) directly below the interface. Consequently, extrinsic doping is unnecessary, and electron sheet densities up to the order of $10^{13}\,cm^{-2}$ can be achieved.[1,2] These special properties make III-nitride materials a key development technology, especially for high-power and high-frequency applications.[3–6]

Non-intentionally doped (nid) GaN layers exhibit n-type background conductivity due to the presence of residual donors, such as Si, O, H, and nitrogen vacancies,[7–11] leading to parallel conduction paths.[5,6,12] To suppress this, a semi-insulating GaN buffer layer is required. The commonly used approach consists of doping the GaN layer with deep acceptors, such as C and Fe, to form compensating acceptor levels.

C-doping in GaN layers can be achieved through extrinsic doping[13–16] or auto-doping,[11,17–21] i.e., by tuning growth conditions, such as low temperature and reduced pressure. This is easily accessible for metal-organic chemical vapor deposition (MOCVD) growth as C is present in the standard precursor (trimethylgallium), although growth with early-stage carbon-free precursors has recently been reported.[22] Auto-doping enables low vertical leakage and high breakdown voltage, which is essential for power-switching applications. Carbon has a self-compensating nature in GaN since it can act as both a donor and acceptor, and for concentrations below $1 \times 10^{19}\,cm^{-3}$, it preferentially occupies a nitrogen site ($C_N \sim E_v + 0.9\,eV$) acting as a deep acceptor.[23] However, the Fermi level is then pinned in the upper half of the bandgap, increasing its susceptibility to dynamic on-resistance and the current collapse effect.[24,25]

Compared to C-doping, Fe-doping can achieve a higher breakdown voltage and lower current collapse in AlGaN/GaN HEMTs.[26] 3d transition metals preferably occupy cation sites in nitrides, and Fe typically sits in a Ga site ($Fe_{Ga} \sim E_c - 0.5\,eV$) as it has the lowest formation energy of all the complexes.[27] Unlike C-doping, Fe-doping is not easily controllable in epitaxial growth, exhibiting a slow turn-off. This effect refers to the incorporation of Fe atoms into subsequently grown layers, even after the flow of its precursor is stopped, through diffusion and/or segregation. Consequently, an Fe "tail" extending to the channel region is observed, leading to trapping effects that limit

© Author(s) 2026

high voltage robustness and long-term reliability. This effect will henceforth be described as dopant "carry-over" into subsequent layers. Growth parameters such as temperature, V/III ratio, and pressure are not sufficient or efficient in reducing the diffusion and/or segregation effects of Fe-doped GaN grown by MOCVD.[28] Several groups have proposed different approaches to mitigate this issue;[29–32] however, it remains a recurring hindrance to device performance.[26,33,34] Due to these effects, at least 500 nm of nid GaN is needed to prevent a severe impact of Fe carry-over on the 2DEGs transport properties.[30,31] Based on Hall measurements, the typical Fe concentration at the GaN channel/AlGaN barrier interface must be below 5×10^{16} cm^{-3}. Arteev *et al.*[31] studied the influence of the doping profile of GaN:Fe buffer layers on the transport properties of AlGaN/GaN HEMTs and observed that reducing the distance between the channel and the Fe-doped buffer by 0.9 μm led to a 10%–20% mobility degradation. Furthermore, their secondary ion mass spectrometry (SIMS) measurements revealed concentrations of Fe in the channel region higher than 10^{17} cm^{-3}. Because both C and Fe have significant drawbacks, alternative dopants for semi-insulating GaN buffers to improve HEMT performance are actively explored.[35–37]

Mn introduces deep levels that pin the Fermi level near GaN's midgap ($Mn^{+2}/Mn^{+3} \sim E_v$+1.42–1.8 eV), effectively compensating residual donors.[38–40] Mn-doping is already used to grow semi-insulating GaN substrates and bulk crystals by ammonothermal and hydride vapor phase epitaxy (HVPE) methods,[41–45] highlighting its potential for highly resistive buffers. Yamamoto *et al.*[35] reported that Mn-doped GaN buffers in AlGaN/GaN HEMTs greatly reduced buffer leakage but caused an on-state drain current drop. The authors suggested that the likely cause was diffusion of Mn into the channel. The ability to precisely incorporate dopants both in concentration and position is critical for device performance. Hence, it is crucial to validate the effectiveness of Mn as a dopant for GaN semi-insulating layers in HEMT heterostructures grown by MOCVD, as it is the industrial standard. Jakiela *et al.*[46] investigated Mn diffusion mechanisms in MOCVD-implanted samples and established the diffusion activation energy as $E_A = 1.8$ eV. Jaroszynska *et al.*[47] studied Mn diffusion in ion-implanted GaN crystals grown by HVPE and reported two mechanisms with distinct parameters. Iso and Izumisawa[48] observed that the Mn diffusion coefficient in GaN grown by HVPE was an order of magnitude higher than that of Fe. While it has been reported that Mn can diffuse from doped GaN substrates into the buffer layers,[49] to the best of our knowledge, there is no study reported yet on the effects of diffusion and segregation for HEMTs with Mn-doped GaN buffer grown by MOCVD. As the contribution of each effect is often unclear, we present two studies of the Mn-doping tail in AlGaN/GaN heterostructures to assess the overall observed carry-over effect of Mn into nid GaN layers. The MOCVD-grown heterostructures were evaluated to ensure smooth morphology, good crystalline quality, and electrical properties for the HEMT structure.

The samples were grown in a commercial multi-wafer, close-coupled showerhead Aixtron MOCVD reactor on 4-in. nominally on-axis semi-insulating 4H-SiC substrates. The standard precursors trimethylaluminum (TMAl) and trimethylgallium (TMGa) were used for Al and Ga, respectively, and ammonia (NH_3) as the N source. Bis(cyclopentadienyl)iron (Cp_2Fe) was chosen as the Fe source, and bis(cyclopentadienyl)manganese (Cp_2Mn) for Mn, whereas in the previous published study by Yamamoto *et al.*,[35] the Mn precursor used was $(EtCp)_2Mn$, which has a higher C-content. H_2 was used as the carrier gas. First, a high-temperature AlN nucleation layer was deposited at 1190 °C, followed by the GaN:Mn and GaN:nid layers grown at 1100 °C with the different configurations exemplified in Fig. 1 and growth rates of 1.3 μm/h. A thin AlGaN barrier layer (~10 nm) with an Al content of 34%–37% was grown on top of the nid GaN layer. The structures were all capped with a thin GaN layer (2 nm).

To explore Mn's doping profile, two different studies were conducted, and consequently, several types of structures were grown:

(1) The Mn-doping level was kept at ~5–6 $\times 10^{17}$ cm^{-3}, and the total stack thickness of the GaN layer (1800 nm) was maintained constant. The thickness of the nid layers varied in each experiment by 100 nm in the range of 100–600 nm, while the Mn-doped layer was changed accordingly to ensure a total stack thickness of 1800 nm [Fig. 1(a)].
(2) The Mn-doping level was changed from a low concentration to high (3×10^{17}, 5×10^{17}, and 1×10^{18} cm^{-3}), with a constant GaN layer thickness, GaN:Mn = 1500 nm and GaN:nid = 300 nm [Fig. 1(b)].

Additionally, samples with Fe-doping were grown for comparison, with a 1.2 μm GaN:Fe layer followed by a GaN:nid layer of 600 nm, with doping levels of 4×10^{17} and 2×10^{18} cm^{-3}.

Mn and Fe concentrations were measured by time-of-flight (ToF) SIMS using an M6 Plus instrument (IONTOF GmbH, Germany). The instrument was operated in the dual-beam mode, using a 30 keV Bi_1^+ primary beam to analyze a 50×50 μm^2 area at the center of a 200×200 μm^2 crater generated by a 1 keV O_2^+ sputter beam. An ion-implanted standard was used to calibrate Fe doping, while a reference sample with a known Mn concentration was used to calibrate Mn-doping. The detection limit of the instrument for both Fe and Mn is approximately 1×10^{15} cm^{-3}. A running average over five data points was applied to all profiles. Crater depths were determined by an integrated scanning probe microscope.

Properties of the crystal layer and strain effects in the structures were assessed with high-resolution X-ray diffractometry (HRXRD) Θ/2Θ-scans of the 0002, 0004, and 0006 reflection ranges combined

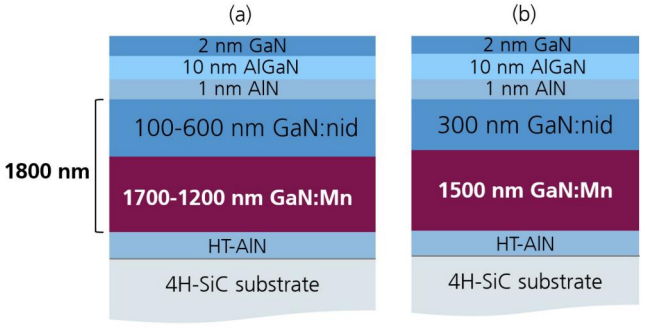

FIG. 1. Schematics of the heterostructures for the different studies: (a) thickness variation at a constant Mn-doping level (~5–6 $\times 10^{17}$ cm^{-3}) and (b) Mn-doping level variation with constant GaN layer thickness.

22 July 2026 14:45:25

© Author(s) 2026

with X-ray reflectometry measured in coplanar geometry of the $11\bar{2}4$ reflection ranges. The structural quality was determined using HRXRD omega scans of the symmetric 0002 and asymmetric $\bar{1}102$ GaN reflections, with the latter measured in skew geometry. A Rigaku SmartLab multipurpose diffractometer system was used for these measurements. Surface morphology was evaluated using the root mean square (RMS) roughness of the samples measured with atomic force microscopy (AFM) in the tapping mode. The measurements were performed in a Bruker Icon instrument.

Room-temperature (RT) contactless Hall-effect and eddy-current sheet resistance measurements on a Semilab LEI tool were used to determine the average values of mobility (μ), carrier density (n_s), and sheet resistance (R_{sh}). The average values were calculated using 17 measurement points evenly distributed across the 4″ wafer. To evaluate the buffer leakage (lateral isolation voltage capability) of the HEMT epitaxial structure based on a Mn-doped GaN buffer (600 nm GaN:Mn with a concentration of 5×10^{17} cm^{-3}), a high voltage bias was applied between two Ohmic contact structures having a width of 200 μm and separations of 3, 5, and 10 μm. The test structures consisted of a Ti/Al/Ni/Au Ohmic metal stack, which was deposited and annealed to form low-resistance Ohmic contacts. Mesa isolation was then performed using a Cl_2 dry etching process to remove the 2DEG conducting channel, reaching an etch depth of approximately 240 nm.

Figure 2 shows a comparison of the ToF-SIMS concentration profile of Fe (gray) and Mn (pink) for two identical heterostructures. For the Mn-doped structure, 200 nm of nid GaN is enough to see the Mn concentration drop in the GaN:nid layer by an order of magnitude, whereas for Fe-doping, 700 nm of nid GaN is needed. Although the Mn profile does not have a sharp interface where the flux of the Mn source is turned off, the observed faster decay may hint at the possibility that the Mn atoms incorporate more easily into the GaN lattice than Fe, thus become less prone to incorporating into the following layers. Bockowski *et al.*[41] reported a similar observation when they doped their bulk HVPE-GaN with Fe. Their source contained an Mn concentration high enough that its concentration in their crystals was, in fact, greater than Fe and suggested that the kinetic barrier of Mn's incorporation into GaN is lower than for Fe. González-Hernández *et al.*[50] investigated the adsorption and diffusion of 3d transition metals by density functional theory and determined that Mn had lower adsorption energies than Fe on the GaN(0001) surface. These two kinetic differences imply a smaller and more rapidly depleted surface reservoir during growth, which may provide a physical explanation for Mn's reduced carry-over. Nevertheless, the complexity of surface thermodynamics and Mn incorporation into the GaN lattice still requires further studies.

Comparing the different nid thicknesses and their concentration profiles (Fig. 3), it can be seen that their behavior is almost identical. In fact, when the profiles are aligned at the GaN:Mn interface, the tail shapes overlap, meaning that the Mn distribution is frozen once the transition from GaN:Mn to GaN:nid occurs, and that the doping tail is tied to the interface itself, unaffected by how much GaN:nid is posteriorly grown. Thus, it appears the Mn incorporation into the GaN:nid layer is dominated by segregation effects, with no observable broadening from Mn diffusion during the subsequent growth.[51] The observed behavior is very likely an incorporation mechanism via surface accumulated layers,[51,52] similar to what is reported by Heikman *et al.*[53] and by Balmer *et al.* for Fe.[28] Analogous to Fe, Mn atoms are not immediately incorporated into the film; instead, they remain at the growth front and are gradually incorporated into the next layers as the flux is switched off. This then creates an exponential-like tail in the growth direction, hitting at a fixed segregation length. While residual donors such as C, O, and Si could affect the observed carry-over effect, given their constant behavior in the depth profiles, these

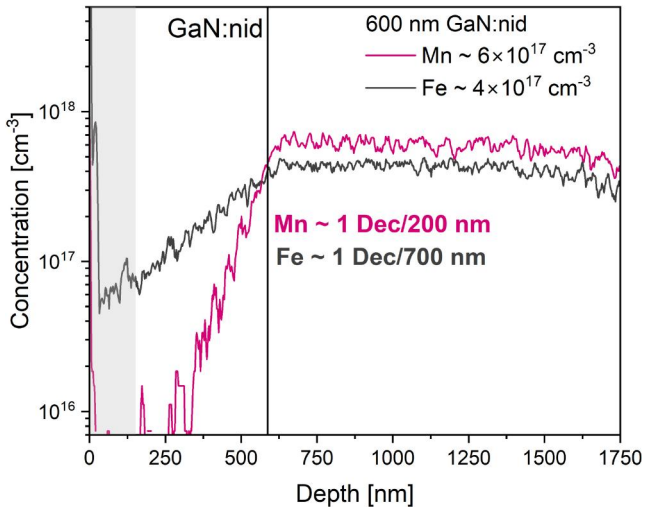

FIG. 2. ToF-SIMS depth profiles of an Fe-doped (gray) and an Mn-doped (pink) heterostructures. The solid line indicates where the doping source is switched off. 1 Dec refers to 1 order of magnitude in concentration of the dopant. The gray shading represents the channel, barrier, and cap. The increase in the Mn signal near the surface is attributed to surface impurities; therefore, it can be neglected. The increase in the Fe signal at a depth of ~18 nm is attributed to the carry-over of Fe into the AlGaN layer. Note that the Fe concentration shown here is not quantitative, as the Fe signal was not calibrated using an AlGaN:Fe standard.

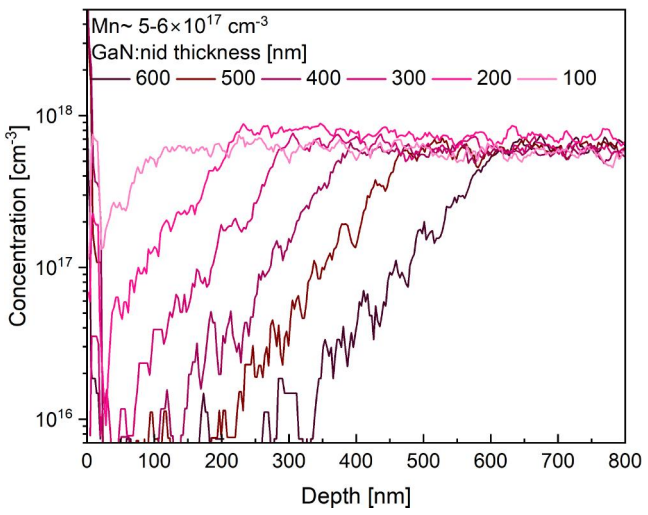

FIG. 3. ToF-SIMS depth profile of the Mn-doped heterostructures with different GaN:nid thicknesses.

22 July 2026 14:45:25

© Author(s) 2026

TABLE I. Electrical characteristics of Mn-doped structures with varying GaN:nid thicknesses, compared with a standard Fe-doped reference structure. Channel concentration refers to its top part.

Doping	GaN:nid (nm)	Channel (cm^{-3})	R_{sh} (Ω/sq)	μ (cm^2/Vs)	n_s ($\times 10^{13}$ cm^{-2})
Fe	600	$\sim 5 \times 10^{16}$	324	1750	1.11
Mn	600	$< 1 \times 10^{15}$	299	1943	1.08
Mn	500	$< 1 \times 10^{15}$	292	1809	1.23
Mn	400	$< 1 \times 10^{15}$	257	1901	1.28
Mn	300	$\sim 1 \times 10^{16}$	266	1945	1.21
Mn	200	$\sim 2 \times 10^{16}$	280	1789	1.26
Mn	100	$\sim 1 \times 10^{17}$	297	1744	1.21

will not have a significant contribution. Further studies to assess the underlying mechanisms are under way, and diffusion effects cannot be completely ruled out.

The samples show adequate RT transport properties (low R_{sh} and high μ and n_{sh}), as present in Table I, with the differences stemming from variations in barrier characteristics. In Fig. 4, it is possible to observe that the high-resistive behavior is indicated by the low leakage current observed for all three contact separations (3, 5, and 10 μm) for a sample with a doping concentration of 5×10^{17} cm^{-3}. The measurement setup (top-left corner of Fig. 4) is designed to assess the buffer isolation of both the remaining GaN:nid layer and the GaN:Mn layer. As shown, the lateral isolation capability reaches 275 and 500 V, with a corresponding absolute leakage current of 50 nA. The observed variation in breakdown voltage is expected to be primarily process-related. All samples presented smooth morphologies, with an RMS roughness below 0.5 nm on the 10×10 μm^2 AFM scans. The crystal quality is confirmed by the HRXRD FWHM of the 0002 and $\bar{1}102$ reflections, $[157 \pm 5]$ arc sec and $[188 \pm 5]$ arc sec, respectively.

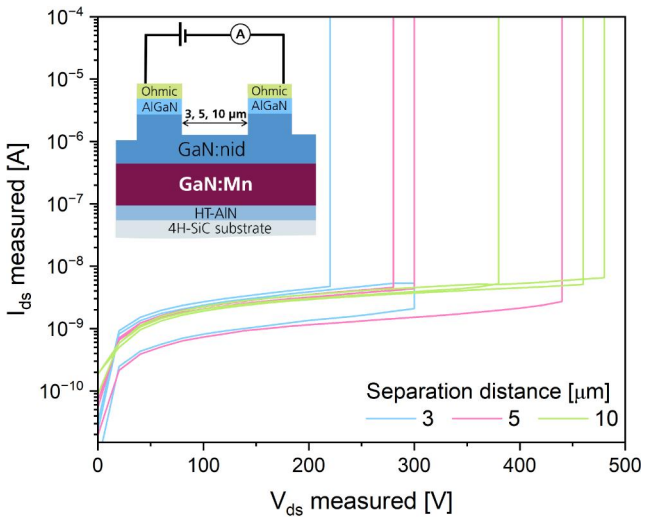

FIG. 4. Lateral isolation voltage capability for a 600 nm GaN:nid structure with a Mn-doped buffer with a concentration of 5×10^{17} cm^{-3} for a width of 200 μm and three separation distances (3, 5, and 10 μm). In the top-left is a schematic of the measurement setup and applied structure.

To investigate the effects of different Mn-doping concentrations on the HEMT epitaxial structures, the thickness of each layer was kept constant, with the GaN:nid layer at 300 nm. By choosing this thickness, it was expected that the Mn concentration in the subsequent layers would not be severe. Additionally, it is thinner than the typical thickness used for our standard Fe-doped GaN buffer layer (500 nm of GaN:nid). Tanaka *et al.*[45] performed a comprehensive study on the electrical properties of semi-insulating GaN substrates with different dopants and concentrations and concluded that with Mn-doping, it was possible to achieve the highest resistivity when using optimized concentrations (8×10^{17} cm^{-3}). It was observed that at very high Mn-doping concentrations, hole conduction is dominant, leading to a monotonic decrease in resistivity. This makes it crucial to use an appropriate doping level. Considering this, three Mn-doping levels were studied: 3×10^{17}, 5×10^{17}, and 1×10^{18} cm^{-3}.

Figure 5(a) shows the concentration profile of Mn in the studied structures. When we offset the ToF-SIMS concentration profiles, the tail shapes overlap again, hinting at the carry-over mechanism previously discussed. The HRXRD omega scans of the symmetric 0002 and asymmetric $\bar{1}102$ reflections at different Mn-doping levels show no significant degradation of the crystal quality of our GaN layers (163 and 180 arc sec, respectively, for the highest Mn-doped structure). Other groups report similar observations for MOCVD-grown GaN with increasingly higher Mn concentration.[35,54] The AFM scans of the structures showed well-defined steps and terraces, with low RMS roughness values (< 0.2 nm on the 10×10 μm^2 scale). Figure 5(b) shows the AFM scan of the structure with the highest Mn-doping level studied (1×10^{18} cm^{-3}).

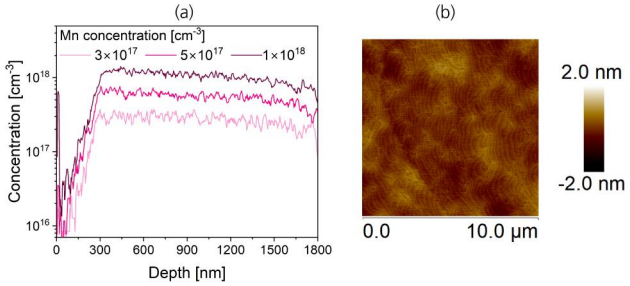

FIG. 5. (a) ToF-SIMS depth profile of the Mn-doped heterostructures with different doping levels. (b) 10×10 μm^2 AFM scan of the high Mn-doping heterostructure (1×10^{18} cm^{-3}) with an RMS roughness of 0.2 nm.

22 July 2026 14:45:25

© Author(s) 2026

TABLE II. Electrical characteristics of Mn-doped structures with varying doping concentration, compared with a standard Fe-doped reference structure. Channel concentration refers to its top part.

Doping	Buffer (cm^{-3})	Channel (cm^{-3})	R_{sh} (Ω/sq)	μ (cm^2/Vs)	n_s ($\times 10^{13}$ cm^{-2})
Fe	2×10^{18}	$\sim 2 \times 10^{17}$	289	1468	1.50
Mn	1×10^{18}	$\sim 2 \times 10^{16}$	269	1844	1.64
Mn	5×10^{17}	$\sim 1 \times 10^{16}$	266	1945	1.21
Mn	3×10^{17}	$< 1 \times 10^{15}$[a]	265	1851	1.28

[a]Below the detection limit.

Yamamoto *et al.*[35] previously explored Mn-doping for GaN buffer layers grown by MOCVD. With this strategy, they reduced the leakage current of their devices by 5 orders of magnitude; however, current collapse was observed during on-state operation. They suggested this phenomenon was due to Mn diffusion, as their SIMS measurements revealed a concentration of 1.5×10^{17} cm^{-3} Mn atoms in the top part of the GaN channel, but no SIMS data were reported. Despite this, we did not observe a similar issue in our heterostructures, as our transport properties did not degrade with Mn-doping (Table II).

The effect of the Mn-doping profile in MOCVD-grown GaN buffer layers was experimentally studied by varying layer thickness and Mn concentration. While Mn exhibited a similar turn-off behavior to Fe, its carry-over was 3.5 times less severe. Having a much faster decay allows for the growth of thinner GaN:nid buffer and channel layers, which may reduce thermal resistance and buffer overheating during device operation. The observed carry-over effect did not degrade transport properties, structural quality, and the morphology of the heterostructures with GaN:nid layers as thin as 100 nm. Mn-doping provides insulating properties with reduced GaN:nid thicknesses compared to conventional Fe-doping while potentially reducing trapping and current collapse. Epitaxial growth of structures for device fabrication and evaluation is ongoing.

The authors thank Christian Manz, Stefan Müller, Hanspeter Menner, and Jannik Richter for their support with sample preparation and characterization. Klaus Köhler is thanked for the valuable scientific discussions and critical reading of the manuscript. This work was conducted as part of the GANYDEM170 project (Project Identification No. 16IPCEI226). The project is supported by the Federal Ministry of Economic Affairs and Energy on the basis of a decision by the German Bundestag. The project is funded by the European Union - NextGenerationEU. The project is sponsored by the Bavarian Ministry of Economic Affairs, Regional Development and Energy. The project is co-funded by the Ministry of Economic Affairs, Industry, Climate Action and Energy of the State of North Rhine-Westphalia.

AUTHOR DECLARATIONS

Conflict of Interest

The authors have no conflicts to disclose.

Author Contributions

Teresa Duarte: Conceptualization (equal); Data curation (equal); Formal analysis (equal); Investigation (equal); Methodology (equal); Visualization (equal); Writing – original draft (equal); Writing – review & editing (equal). **Patrik Straňák:** Formal analysis (supporting); Investigation (supporting); Writing – review & editing (supporting). **Lutz Kirste:** Formal analysis (supporting); Investigation (supporting); Writing – review & editing (supporting). **Mario Prescher:** Formal analysis (supporting); Investigation (supporting); Writing – review & editing (supporting). **Fouad Benkhelifa:** Formal analysis (supporting); Investigation (supporting); Writing – review & editing (supporting). **Byeongchan So:** Conceptualization (equal); Data curation (equal); Formal analysis (equal); Investigation (equal); Project administration (equal); Resources (equal); Supervision (equal); Validation (equal); Writing – review & editing (equal). **Stefano Leone:** Conceptualization (equal); Data curation (equal); Formal analysis (equal); Funding acquisition (equal); Investigation (equal); Project administration (equal); Resources (equal); Supervision (equal); Validation (equal); Writing – review & editing (equal). **Patricie Merkert:** Funding acquisition (lead); Resources (lead); Writing – review & editing (supporting). **Rüdiger Quay:** Funding acquisition (lead); Resources (lead); Supervision (lead); Writing – review & editing (supporting).

DATA AVAILABILITY

The data that support the findings of this study are available from the corresponding authors upon reasonable request.

REFERENCES

[1]O. Ambacher, J. Smart, J. R. Shealy, N. G. Weimann, K. Chu, M. Murphy, W. J. Schaff, L. F. Eastman, R. Dimitrov, L. Wittmer, M. Stutzmann, W. Rieger, and J. Hilsenbeck, "Two-dimensional electron gases induced by spontaneous and piezoelectric polarization charges in N- and Ga-face AlGaN/GaN heterostructures," J. Appl. Phys. **85**, 3222–3233 (1999).
[2]O. Ambacher, J. Majewski, C. Miskys, A. Link, M. Hermann, M. Eickhoff, M. Stutzmann, F. Bernardini, V. Fiorentini, V. Tilak, B. Schaff, and L. F. Eastman, "Pyroelectric properties of Al(In)GaN/GaN hetero- and quantum well structures," J. Phys.: Condens. Matter **14**, 3399 (2002).
[3]R. Trew, G. Bilbro, W. Kuang, Y. Liu, and H. Yin, "Microwave AlGaN/GaN HFETs," IEEE Microwave Mag. **6**, 56–66 (2005).
[4]E. A. Jones, F. F. Wang, and D. Costinett, "Review of commercial GaN power devices and GaN-based converter design challenges," IEEE J. Emerg. Sel. Top. Power Electron. **4**, 707–719 (2016).
[5]H. Amano, Y. Baines, E. Beam, M. Borga, T. Bouchet, P. R. Chalker, M. Charles, K. J. Chen, N. Chowdhury, R. Chu, C. De Santi, M. M. De Souza, S. Decoutere, L. Di Cioccio, B. Eckardt, T. Egawa, P. Fay, J. J. Freedsman, L. Guido, O. Häberlen, G. Haynes, T. Heckel, D. Hemakumara, P. Houston, J. Hu, M. Hua, Q. Huang, A. Huang, S. Jiang, H. Kawai, D. Kinzer, M. Kuball, A. Kumar, K. B. Lee, X. Li, D. Marcon, M. März, R. McCarthy, G. Meneghesso, M. Meneghini, E. Morvan, A. Nakajima, E. M. S. Narayanan, S.

22 July 2026 14:45:25

© Author(s) 2026

Oliver, T. Palacios, D. Piedra, M. Plissonnier, R. Reddy, M. Sun, I. Thayne, A. Torres, N. Trivellin, V. Unni, M. J. Uren, M. Van Hove, D. J. Wallis, J. Wang, J. Xie, S. Yagi, S. Yang, C. Youtsey, R. Yu, E. Zanoni, S. Zeltner, and Y. Zhang, "The 2018 GaN power electronics roadmap," J. Phys. D **51**, 163001 (2018).
[6]K. Hoo Teo, Y. Zhang, N. Chowdhury, S. Rakheja, R. Ma, Q. Xie, E. Yagyu, K. Yamanaka, K. Li, and T. Palacios, "Emerging GaN technologies for power, RF, digital, and quantum computing applications: Recent advances and prospects," J. Appl. Phys. **130**, 160902 (2021).
[7]C. Wetzel, T. Suski, J. W. Ager III, E. R. Weber, E. E. Haller, S. Fischer, B. K. Meyer, R. J. Molnar, and P. Perlin, "Pressure induced deep gap state of oxygen in GaN," Phys. Rev. Lett. **78**, 3923–3926 (1997).
[8]C. Y. Hwang, M. J. Schurman, W. E. Mayo, Y. C. Lu, R. A. Stall, and T. Salagaj, "Effect of structural defects and chemical impurities on hall mobilities in low pressure MOCVD grown GaN," J. Electron. Mater. **26**, 243–251 (1997).
[9]M. G. Cheong, K. S. Kim, C. S. Oh, N. W. Namgung, G. M. Yang, C.-H. Hong, K. Y. Lim, E.-K. Suh, K. S. Nahm, H. J. Lee, D. H. Lim, and A. Yoshikawa, "Conductive layer near the GaN/sapphire interface and its effect on electron transport in unintentionally doped n-type GaN epilayers," Appl. Phys. Lett. **77**, 2557–2559 (2000).
[10]W. J. Moore, J. A. Freitas, Jr., G. C. B. Braga, R. J. Molnar, S. K. Lee, K. Y. Lee, and I. J. Song, "Identification of Si and O donors in hydride-vapor-phase epitaxial GaN," Appl. Phys. Lett. **79**, 2570–2572 (2001).
[11]D. D. Koleske, A. E. Wickenden, R. L. Henry, and M. E. Twigg, "Influence of MOVPE growth conditions on carbon and silicon concentrations in GaN," J. Cryst. Growth **242**, 55–69 (2002).
[12]V. Desmaris, M. Rudzinski, N. Rorsman, P. Hageman, P. Larsen, H. Zirath, T. Rodle, and H. Jos, "Comparison of the DC and microwave performance of AlGaN/GaN HEMTs grown on SiC by MOCVD with Fe-doped or unintentionally doped GaN buffer layers," IEEE Trans. Electron Devices **53**, 2413–2417 (2006).
[13]X. Li, J. Bergsten, D. Nilsson, Ö Danielsson, H. Pedersen, N. Rorsman, E. Janzén, and U. Forsberg, "Carbon doped GaN buffer layer using propane for high electron mobility transistor applications: Growth and device results," Appl. Phys. Lett. **107**, 262105 (2015).
[14]X. Li, Ö Danielsson, H. Pedersen, E. Janzén, and U. Forsberg, "Precursors for carbon doping of GaN in chemical vapor deposition," J. Vac. Sci. Technol., B **33**, 021208 (2015).
[15]J. Bergsten, X. Li, D. Nilsson, Ö Danielsson, H. Pedersen, E. Janzén, U. Forsberg, and N. Rorsman, "AlGaN/GaN high electron mobility transistors with intentionally doped GaN buffer using propane as carbon precursor," Jpn. J. Appl. Phys. **55**, 05FK02 (2016).
[16]H. Yacoub, C. Mauder, S. Leone, M. Eickelkamp, D. Fahle, M. Heuken, H. Kalisch, and A. Vescan, "Effect of different carbon doping techniques on the dynamic properties of GaN-on-Si buffers," IEEE Trans. Electron Devices **64**, 991–997 (2017).
[17]G. Parish, S. Keller, S. P. Denbaars, and U. K. Mishra, "SIMS investigations into the effect of growth conditions on residual impurity and silicon incorporation in GaN and $Al_xGa_{1-x}N$," J. Electron. Mater. **29**, 15–20 (2000).
[18]C. H. Seager, A. F. Wright, J. Yu, and W. Götz, "Role of carbon in GaN," J. Appl. Phys. **92**, 6553–6560 (2002).
[19]A. Armstrong, A. R. Arehart, B. Moran, S. P. DenBaars, U. K. Mishra, J. S. Speck, and S. A. Ringel, "Impact of carbon on trap states in n-type GaN grown by metalorganic chemical vapor deposition," Appl. Phys. Lett. **84**, 374–376 (2004).
[20]A. E. Wickenden, D. D. Koleske, R. L. Henry, M. E. Twigg, and M. Fatemi, "Resistivity control in unintentionally doped GaN films grown by MOCVD," J. Cryst. Growth **260**, 54–62 (2004).
[21]S. Kato, Y. Satoh, H. Sasaki, I. Masayuki, and S. Yoshida, "C-doped GaN buffer layers with high breakdown voltages for high-power operation AlGaN/GaN HFETs on 4-in Si substrates by MOVPE," J. Cryst. Growth **298**, 831–834 (2007).
[22]S. Leone, T. Duarte, H. Menner, J. Richter, L. Kirste, S. Maegdefessel, F. Hoffmann, B. So, and R. Quay, "Chemical vapor deposition of nitrides by carbon-free brominated precursors," Phys. Status Solidi (a) **223**, e202600005 (2026).
[23]J. L. Lyons, A. Janotti, and C. G. Van de Walle, "Effects of carbon on the electrical and optical properties of InN, GaN, and AlN," Phys. Rev. B **89**, 035204 (2014).
[24]M. J. Uren, J. Moreke, and M. Kuball, "Buffer design to minimize current collapse in GaN/AlGaN HFETs," IEEE Trans. Electron Devices **59**, 3327–3333 (2012).
[25]J. Würfl, O. Hilt, E. Bahat-Treidel, R. Zhytnytska, P. Kotara, F. Brunner, O. Krueger, and M. Weyers, "Techniques towards GaN power transistors with improved high voltage dynamic switching properties," in *2013 IEEE International Electron Devices Meeting* (IEEE, 2013), pp. 6.1.1–6.1.4.
[26]O. Axelsson, S. Gustafsson, H. Hjelmgren, N. Rorsman, H. Blanck, J. Splettstoesser, J. Thorpe, T. Roedle, and M. Thorsell, "Application relevant evaluation of trapping effects in AlGaN/GaN HEMTs with Fe-doped buffer," IEEE Trans. Electron Devices **63**, 326–332 (2016).
[27]D. Wickramaratne, "Electrical and optical properties of iron in GaN, AlN, and InN," Phys. Rev. B **99**, 205202 (2019).
[28]R. S. Balmer, D. E. J. Soley, A. J. Simons, J. D. Mace, L. Koker, P. O. Jackson, D. J. Wallis, M. J. Uren, and T. Martin, "On the incorporation mechanism Fe in GaN grown by metal-organic vapour phase epitaxy," phys. status solidi c **3**, 1429–1434 (2006).
[29]T. Ishiguro, A. Yamada, J. Kotani, N. Nakamura, T. Kikkawa, K. Watanabe, and K. Imanishi, "New model of Fe diffusion in highly resistive Fe-doped buffer layer for GaN high-electron-mobility transistor," Jpn. J. Appl. Phys. **52**, 08JB17 (2013).
[30]S. Leone, F. Benkhelifa, L. Kirste, C. Manz, S. Mueller, R. Quay, and T. Stadelmann, "Suppression of iron memory effect in GaN epitaxial layers," Phys. Status Solidi (b) **255**, 1700377 (2018).
[31]D. S. Arteev, A. V. Sakharov, W. V. Lundin, E. E. Zavarin, D. A. Zakheim, A. F. Tsatsulnikov, M. I. Gindina, and P. N. Brunkov, "Influence of doping profile of GaN:Fe buffer layer on the properties of AlGaN/AlN/GaN heterostructures for high-electron mobility transistors," J. Phys.: Conf. Ser. **1697**, 012206 (2020).
[32]J.-J. Dai, T. T. Mai, U. R. Nallasani, S.-C. Chang, H.-I. Hsiao, S.-K. Wu, C.-W. Liu, H.-C. Wen, W.-C. Chou, C.-P. Wang, and L. H. Hoang, "The effect of heavy Fe-doping on 3D growth mode and Fe diffusion in GaN for high power HEMT application," Materials **15**, 2058 (2022).
[33]Y. S. Puzyrev, R. D. Schrimpf, D. M. Fleetwood, and S. T. Pantelides, "Role of Fe impurity complexes in the degradation of GaN/AlGaN high-electron-mobility transistors," Appl. Phys. Lett. **106**, 053505 (2015).
[34]M. Meneghini, C. De Santi, I. Abid, M. Buffolo, M. Cioni, R. A. Khadar, L. Nela, N. Zagni, A. Chini, F. Medjdoub *et al.*, "GaN-based power devices: Physics, reliability, and perspectives," J. Appl. Phys. **130**, 181101 (2021).
[35]T. Yamamoto, H. Sazawa, N. Nishikawa, M. Kiuchi, T. Ide, M. Shimizu, T. Inoue, and M. Hata, "Reduction in buffer leakage current with Mn-doped GaN buffer layer grown by metal organic chemical vapor deposition," Jpn. J. Appl. Phys. **52**, 08JN12 (2013).
[36]H. Ahmad, T. J. Anderson, J. C. Gallagher, E. A. Clinton, Z. Engel, C. M. Matthews, and W. Alan Doolittle, "Beryllium doped semi-insulating GaN without surface accumulation for homoepitaxial high power devices," J. Appl. Phys. **127**, 215703 (2020).
[37]K. Ko, K. Lee, B. So, C. Heo, K. Lee, T. Kwak, S.-W. Han, H.-Y. Cha, and O. Nam, "Mg-compensation effect in GaN buffer layer for AlGaN/GaN high-electron-mobility transistors grown on 4H-SiC substrate," Jpn. J. Appl. Phys. **56**, 015502 (2017).
[38]L. Janicki, G. Kunert, M. Sawicki, E. Piskorska-Hommel, K. Gas, R. Jakiela, D. Hommel, and R. Kudrawiec, "Fermi level and bands offsets determination in insulating (Ga,Mn)N/GaN structures," Sci. Rep. **7**, 41877 (2017).
[39]R. Y. Korotkov, J. M. Gregie, and B. W. Wessels, "Optical properties of the deep Mn acceptor in GaN:Mn," Appl. Phys. Lett. **80**, 1731–1733 (2002).
[40]T. Graf, M. Gjukic, M. S. Brandt, M. Stutzmann, and O. Ambacher, "The $Mn^{3+/2+}$ acceptor level in group III nitrides," Appl. Phys. Lett. **81**, 5159–5161 (2002).
[41]M. Bockowski, M. Iwinska, M. Amilusik, B. Lucznik, M. Fijalkowski, E. Litwin-Staszewska, R. Piotrzkowski, and T. Sochacki, "Doping in bulk HVPE-GaN grown on native seeds – highly conductive and semi-insulating crystals," J. Cryst. Growth **499**, 1–7 (2018).
[42]M. Iwinska, M. Zajac, B. Lucznik, M. Fijalkowski, M. Amilusik, T. Sochacki, E. Litwin-Staszewska, R. Piotrzkowski, I. Grzegory, and M. Bockowski, "Iron and manganese as dopants used in the crystallization of highly resistive HVPE-GaN on native seeds," Jpn. J. Appl. Phys. **58**, SC1047 (2019).

22 July 2026 14:45:25

© Author(s) 2026

[43]M. Amilusik, M. Zajac, T. Sochacki, B. Lucznik, M. Fijalkowski, M. Iwinska, D. Wlodarczyk, A. K. Somakumar, A. Suchocki, and M. Bockowski, "Carbon and manganese in semi-insulating bulk GaN crystals," Materials **15**, 2379 (2022).
[44]K. Iso, H. Ikeda, T. Mochizuki, T. Odani, and S. Izumisawa, "Dual-layer semi-insulating GaN substrates doped with Fe, C, or Mn," Phys. Status Solidi (b) **260**, 2200489 (2023).
[45]D. Tanaka, K. Iso, and J. Suda, "Comparative study of electrical properties of semi-insulating GaN substrates grown by hydride vapor phase epitaxy and doped with Fe, C, or Mn," J. Appl. Phys. **133**, 055701 (2023).
[46]R. Jakiela, K. Gas, M. Sawicki, and A. Barcz, "Diffusion of Mn in gallium nitride: Experiment and modelling," J. Alloys Compd. **771**, 215–220 (2019).
[47]A. Jaroszynska, K. Sierakowski, R. Jakiela, M. Turek, M. Fijalkowski, T. Sochacki, and M. Bockowski, "Ultra-high pressure annealing of Mn-implanted HVPE-GaN," J. Alloys Compd. **966**, 171612 (2023).
[48]K. Iso and S. Izumisawa, "Diffusion of acceptor metal impurities from semi-insulating GaN into undoped GaN epitaxial layers," Phys. Status Solidi (b) **262**, 2500021 (2025).
[49]D. Tanaka, K. Iso, R. Makisako, Y. Ando, and J. Suda, "Electrical characterization of AlGaN/GaN-HEMTs on semi-insulating GaN substrates doped with Fe, C, or Mn and grown by hydride vapor phase epitaxy," IEEE Trans. Electron Devices **71**, 3096–3101 (2024).
[50]R. González-Hernández, W. López-Pérez, M. Guadalupe Moreno-Armenta, and M. J. Arbey Rodríguez, "Adsorption and diffusion of 3d transition metal atoms on the GaN(0001) surface," J. Appl. Phys. **110**, 083712 (2011).
[51]K. Muraki, S. Fukatsu, Y. Shiraki, and R. Ito, "Surface segregation of In atoms during molecular beam epitaxy and its influence on the energy levels in InGaAs/GaAs quantum wells," Appl. Phys. Lett. **61**, 557–559 (1992).
[52]K. Köhler, R. Gutt, J. Wiegert, and L. Kirste, "Diffusion of Mg dopant in metal-organic vapor-phase epitaxy grown GaN and $Al_xGa_{1-x}N$," J. Appl. Phys. **113**, 073514 (2013).
[53]S. Heikman, S. Keller, T. Mates, S. P. DenBaars, and U. K. Mishra, "Growth and characteristics of Fe-doped GaN," J. Cryst. Growth **248**, 513–517 (2003).
[54]X. G. Cui, Z. K. Tao, R. Zhang, X. Li, X. Q. Xiu, Z. L. Xie, S. L. Gu, P. Han, Y. Shi, and Y. D. Zheng, "Structural and magnetic properties in Mn-doped GaN grown by metal organic chemical vapor deposition," Appl. Phys. Lett. **92**, 152116 (2008).

22 July 2026 14:45:25

© Author(s) 2026